

# Four-nucleon system with $\Delta$ -isobar excitation

A. Deltuva<sup>a</sup>, A. C. Fonseca<sup>a</sup>, P. U. Sauer<sup>b</sup>

<sup>a</sup>*Centro de Física Nuclear da Universidade de Lisboa, P-1649-003 Lisboa, Portugal*

<sup>b</sup>*Institut für Theoretische Physik, Leibniz Universität Hannover, D-30167 Hannover, Germany*

---

## Abstract

The four-nucleon bound state and scattering below three-body breakup threshold are described based on the realistic coupled-channel potential CD Bonn +  $\Delta$  which allows the excitation of a single nucleon to a  $\Delta$  isobar. The Coulomb repulsion between protons is included. In the four-nucleon system the two-baryon coupled-channel potential yields effective two-, three- and four-nucleon forces, mediated by the  $\Delta$  isobar and consistent with each other and with the underlying two-nucleon force. The effect of the four-nucleon force on the studied observables is much smaller than the effect of the three-nucleon force. The inclusion of the  $\Delta$  isobar is unable to resolve the existing discrepancies with the experimental data.

*Key words:* Four-nucleon, bound state, scattering,  $\Delta$ -isobar, many-nucleon forces

*PACS:* 21.45.+v, 21.30.-x, 24.70.+s, 25.10.+s

---

## 1. Introduction

State of art calculations of four-nucleon ( $4N$ ) scattering have been recently presented in Refs. [1,2,3] for all possible reactions initiated by  $n$ - $^3\text{H}$ ,  $p$ - $^3\text{He}$ ,  $n$ - $^3\text{He}$ ,  $p$ - $^3\text{H}$  and  $d$ - $d$  below three-body breakup threshold. Realistic two-nucleon ( $2N$ ) interactions based on meson theory like AV18 [4], CD Bonn [5] and INOY04 [6] or chiral effective field theory (EFT) [7] are used between pairs together with the Coulomb repulsion between the protons. No approximations were used in the solution of the four-body scattering equations beyond the usual partial-wave decomposition and the discretization of integration variables. The results presented are fully converged vis-a-vis the included partial waves as well as the number of mesh points used for the discretization of all continuous variables. Some observables we obtain are described quite well by all interaction models, some scale with the three-nucleon ( $3N$ ) binding energy, and some show large deviations from the data.

Therefore the next step in our understanding of  $4N$  observables in terms of the underlying forces between nucleons requires the inclusion of a  $3N$  force. There are three distinct ways for doing this: a) Add a static two-pion-exchange irreducible  $3N$  force [8,9,10] to the underlying  $2N$  forces; however, in this approach these two forces are not really consistent with each other. b) Use  $2N + 3N$  force models based

on chiral EFT [11,12] to guaranty consistency between the  $2N$  and  $3N$  forces; however, for a realistic description, the expansion up to at least next-to-next-to-next-to leading order (N<sup>3</sup>LO) is required, which for the  $3N$  force is not yet available. c) Extend the purely nucleonic model to allow the explicit excitation of a nucleon ( $N$ ) to a  $\Delta$  isobar as was carried out in Ref. [13] for the  $2N$  and  $3N$  systems; this approach yields effective many-nucleon forces consistent with the underlying  $2N$  force, but does not fully satisfy chiral symmetry, much like a).

The studies of the  $3N$  system reveal that all these different approaches lead to qualitatively similar results. In the  $4N$  system the first one a) was already applied to  $n$ - $^3\text{H}$  [14,15] and  $p$ - $^3\text{He}$  [16,17] scattering. In the present paper, following the work on the  $3N$  system performed in Refs.[13,18,19], we use the last approach c) to study all  $4N$  reactions below three-body breakup threshold. In the  $3N$  system the excitation of a single nucleon to a  $\Delta$  isobar yields an effective  $3N$  force with components of Fujita-Miyazawa type [20] and much richer structures in a reducible form; beside pion ( $\pi$ ) exchange, the  $3N$  force has contributions of shorter range due to the exchange of heavier mesons. In the  $4N$  system an effective  $4N$  force arises that also has parts of shorter range than  $\pi$  exchange.

The paper introduces the dynamics chosen for the extended description of the  $4N$  system in Section 2. It discusses the effects of  $\Delta$ -isobar excitation in the form of  $3N$  and  $4N$  forces on the  $4N$  bound state in Section 3 and on

---

*Email address:* [deltuva@cii.fc.ul.pt](mailto:deltuva@cii.fc.ul.pt) (A. Deltuva).

low-energy  $4N$  scattering observables in Section 4. Conclusions are given in Section 5.

## 2. Dynamics

The description of the  $4N$  system is given in a Hilbert space consisting of two sectors as depicted in Fig. 1; the first sector  $\mathcal{H}_N$  is purely nucleonic, and in the second sector  $\mathcal{H}_\Delta$  one nucleon is replaced by a  $\Delta$  isobar of mass  $m_\Delta = 1232$  MeV. The restriction to Hilbert sectors with one  $\Delta$  at most has a strong physics motivation. The single  $\Delta$  isobar, when coupled to explicit pion-nucleon states, mediates the  $P_{33}$  resonance in pion-nucleon scattering; it also mediates single-pion production in  $2N$  scattering where single-pion production is the dominant inelastic channel up to about 500 MeV in the  $2N$  center of mass (c.m.) system, i.e., far beyond the two-pion threshold. Thus, the adopted Hilbert space is sufficient for a further extension to the intermediate-energy pionic channels where a Hilbert sector with two pions appears to be dynamically suppressed. The nucleons in the sector  $\mathcal{H}_N$  are fully antisymmetrized. The sector  $\mathcal{H}_\Delta$  does not have a physics life on its own, but is included only through its coupling to  $\mathcal{H}_N$ . That coupling is symmetric in all nucleons. Though the  $\Delta$  isobar is physically distinct from the nucleons, only wavefunction components, antisymmetrized in all four baryons, nucleons and the  $\Delta$  isobar, have to be considered. Thus, Faddeev-Yakubovsky bound-state equations in the symmetrized form of Ref. [21] and Alt, Grassberger and Sandhas (AGS) scattering equations [22] in the symmetrized form of Refs. [1,2,3] can be used.

The dynamics is specified by a hermitian Hamiltonian  $H$  with instantaneous two-baryon potentials as indicated in Fig. 2 for the  $4N$  system. The Hamiltonian acts in both Hilbert sectors  $\mathcal{H}_N$  and  $\mathcal{H}_\Delta$  and couples them. The hermitian-conjugate of the component (b) is not shown separately. When limited to the  $2N$  system, the Hamiltonian of Fig. 2 (a) - (c), i.e., its respective components  $v_{NN}$ ,  $v_{\Delta N} = v_{N\Delta}^\dagger$  and  $v_{\Delta\Delta}$ , reduces to the potential CD Bonn +  $\Delta$ , a realistic coupled-channel two-baryon potential, fitted in Ref. [13] to the elastic  $2N$  data. The Hamiltonian component of Fig. 2 (d), corresponding to the  $2N$  potential in the presence of a  $\Delta$  isobar, is not constrained by  $2N$  data. A reasonable choice is the purely nucleonic CD Bonn potential [5] which we used in our previous  $3N$  calculations. However, we found that the results for  $3N$  observables depend extremely weakly on the parametrization of the

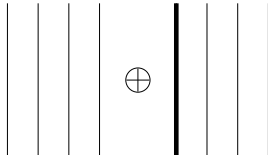


Fig. 1. Four-baryon Hilbert space considered. It consists of a purely nucleonic sector  $\mathcal{H}_N$  and a sector  $\mathcal{H}_\Delta$  in which one nucleon is turned into a  $\Delta$  isobar, indicated by a thick line.

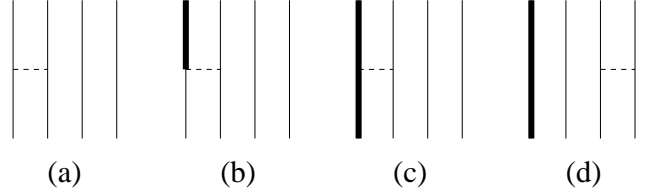


Fig. 2. Four-baryon Hamiltonian. The dashed horizontal lines indicate potentials.

potential in Fig. 2 (d). Even choosing it to be zero has no visible consequences on the description of  $3N$  observables; e.g., the calculated  $3N$  binding energy changes by 20 keV only. Therefore we choose the Hamiltonian component of Fig. 2 (d) to be zero in our  $4N$  calculations. That choice is an assumption on unknown dynamics, but it also yields a technical simplification. The solution of the  $4N$  equations remains exact.

### 2.1. Equations

The symmetrized equations for the Faddeev-Yakubovsky amplitudes  $|\psi_\alpha\rangle$  of the  $4N$  bound state are

$$|\psi_1\rangle = G_0 T G_0 U_1 (-P_{34} |\psi_1\rangle + |\psi_2\rangle), \quad (1a)$$

$$|\psi_2\rangle = G_0 T G_0 U_2 (1 - P_{34}) |\psi_1\rangle, \quad (1b)$$

where  $G_0$  is the free four-particle Green's function and  $T$  the two-baryon transition matrix. The operators  $U_\alpha$  obtained from

$$U_\alpha = P_\alpha G_0^{-1} + P_\alpha T G_0 U_\alpha, \quad (2a)$$

$$P_1 = P_{12} P_{23} + P_{13} P_{23}, \quad (2b)$$

$$P_2 = P_{13} P_{24}, \quad (2c)$$

are the symmetrized AGS operators for the  $1+3$  and  $2+2$  subsystems and  $P_{ij}$  is the permutation operator of particles  $i$  and  $j$ . The equations suffice for calculating the binding energy. The step from the Faddeev-Yakubovsky amplitudes  $|\psi_\alpha\rangle$  to the bound state wave function is not yet carried out.

The corresponding equations for  $4N$  scattering and the description of the screening and renormalization method to include the Coulomb interaction are given in Refs. [1,2,3], and for that reason are not repeated here.

### 2.2. The isolation of $\Delta$ -isobar effects

Full four-body calculations are carried out in Section 3 for the  $4N$  bound state and in Section 4 for selected  $4N$  reactions. The dynamics is based on the coupled-channel potential CD Bonn +  $\Delta$ ; the purely nucleonic CD Bonn potential serves as reference for isolating the full  $\Delta$ -isobar effect on the considered observables. However, a split of the total  $\Delta$ -isobar effect into separate contributions is highly desirable for understanding the physics of the results. For this goal a sequence of incomplete calculations is also done. The dynamic input, the coupled-channel two-baryon transition matrix is calculated correctly in all its components

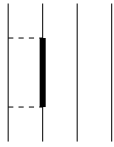


Fig. 3. Lowest order contribution to the  $2N$  dispersion.

$T_{NN}$ ,  $T_{\Delta N}$ ,  $T_{N\Delta}$ , and  $T_{\Delta\Delta}$ , but is only partially included in the following incomplete calculations:

(1) Only the purely nucleonic component  $T_{NN}$  of the two-baryon transition matrix is retained. The lowest order  $\Delta$  contribution to the dynamics, kept in this calculation, is shown in Fig. 3. It renders the  $2N$  interaction less attractive off-shell. This is the well known effect of  $2N$  dispersion.

(2) Only the two-baryon transition matrix components  $T_{NN}$ ,  $T_{\Delta N}$ , and  $T_{N\Delta}$  are retained. The most important  $\Delta$  contribution to the dynamics, kept in this calculation in addition to the  $2N$  dispersion, is of Fujita-Miyazawa (FM) type shown in Fig. 4 together with higher order  $3N$  force contributions; the sample process on the right-hand side of Fig. 4 occurs due to two-body contributions contained in  $T_{N\Delta}$ . However, according to Ref. [23], those higher order  $3N$  force contributions should be far less important. Thus, the second incomplete calculation, when compared to the first one, is a reasonable estimation for the effective  $3N$  force of the Fujita-Miyazawa type.

(3) In the third incomplete calculation all  $4N$  force effects are attempted to be eliminated while keeping all  $3N$  force effects. The two-baryon transition matrix component  $T_{\Delta\Delta}$ , contained in the  $1 + 3$  subsystem transition operator  $U_1$ , generates higher order (h.o.)  $3N$  force contributions like those in Fig. 5, in which one spectating nucleon is interaction-free. In addition, due to the purely nucleonic intermediate states in  $T_{\Delta\Delta}$ , even particular iterations of the  $3N$  Fujita-Miyazawa force are generated like the one also shown in Fig. 5, in which all four baryons are involved in the interaction process. But  $T_{\Delta\Delta}$  is also the source for the effective  $4N$  force, whose corresponding lowest order contributions are shown in Fig. 6. The clean elimination of the  $4N$  force is achieved by using the full  $T_{\Delta\Delta}$  component in the calculation of  $U_1$ , but the modified part  $T_{\Delta\Delta} - T'_{\Delta\Delta}$  when the transition matrix acts immediately before/after the permutation operator  $P_{34}$  in the iteration process of Eq. (1a) where the particular transition matrix to be modified occurs explicitly. The subtraction of  $T'_{\Delta\Delta} = v_{\Delta\Delta}(1 + G_0 T'_{\Delta\Delta})$  ensures the presence of the purely nucleonic intermediate state between two successive  $3N$  transition operators  $U_1$ , which act, due to the permutation  $P_{34}$ , in different  $3N$  subsystems. It therefore eliminates all  $4N$  force contributions for which Fig. 6 gives lowest order examples. Thus, when comparing this calculation to the previous incomplete calculation (2) and to the full calculation, the effects of h. o.  $3N$  force contributions and of the  $4N$  force are estimated separately.

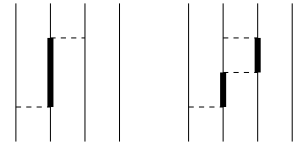


Fig. 4. Effective  $3N$  force of the Fujita-Miyazawa type (left side) and an example for a higher order  $3N$  force (right side) that is included together.

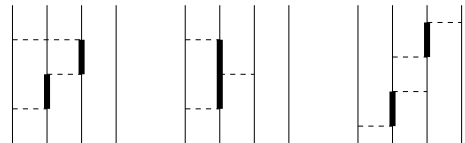


Fig. 5. Examples for higher order  $3N$  force processes. The first two diagrams show contributions to the  $3N$  force mediated by the two-baryon transition matrix component  $T_{\Delta\Delta}$  contained in  $U_1$ ; one nucleon stays uninvolved. In the last diagram all four nucleons interact; the process is the iteration of the  $3N$  Fujita-Miyazawa force; it is due to the purely nucleonic intermediate states in  $T_{\Delta\Delta}$ .

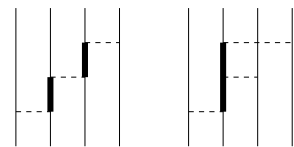


Fig. 6. Lowest order effective  $4N$  force contributions.

### 3. Four-nucleon bound state

In the present study the binding energy for the  $4N$  bound state is calculated. Other properties, such as the charge radius or the charge form factor, are not determined yet. Only total isospin  $\mathcal{T} = 0$  states are included and isospin averaging is performed for the two-baryon transition matrix.

In Table 1 we collect the results for  $3N$  and  $4N$  binding energies. The inclusion of the  $\Delta$  isobar increases the corresponding binding energies but is unable to reproduce the experimental values. Obviously, many-nucleon forces, not accounted for by the  $\Delta$  isobar, make a rather significant contribution to  $3N$  and  $4N$  binding energies. Table 1 also splits up the total  $\Delta$ -isobar effect into separate contributions obtained through incomplete calculations as discussed in Section 2.2. (1) The  $2N$  dispersion turns out to be massive in the  $4N$  bound state with  $\Delta E_2 = -2.80$  MeV; it arises mainly from the dispersion in the  $^1S_0$   $2N$  partial wave. (2) The  $3N$  force contribution of the Fujita-Miyazawa type  $\Delta E_3^{\text{FM}} = 2.25$  MeV is also quite large. The increase by the factor of 4.5 compared to the  $3N$  bound state is understandable in terms of the different multiplicity with which the  $3N$  force contributes: one in the  $3N$  bound state and four in the  $4N$ . The observed factor of  $\approx 4.5$  comes from the fact that  $^4\text{He}$ , being a denser system than  $^3\text{He}$  or  $^3\text{H}$ , squeezes out more binding from the underlying force. (3) The contribution of the higher order  $3N$  force terms mediated by the diagonal  $N\Delta$  potential  $v_{\Delta\Delta}$  is  $\Delta E_3^{\text{h.o.}} = 1.30$  MeV comparable to the one of the Fujita-Miyazawa type. The size of these h. o. terms depends on the strength of

	${}^3\text{H}$	${}^3\text{He}$	${}^4\text{He}$
CD Bonn	8.00	7.26	26.18
CD Bonn + $\Delta$	8.28	7.53	27.10
exp	8.48	7.72	28.30
$\Delta E_2$	-0.51	-0.48	-2.80
$\Delta E_3^{\text{FM}}$	0.50	0.48	2.25
$\Delta E_3^{\text{h.o.}}$	0.29	0.27	1.30
$\Delta E_4$			0.17

Table 1

Binding energies for  ${}^3\text{H}$ ,  ${}^3\text{He}$ , and  ${}^4\text{He}$  derived from the potentials CD Bonn and CD Bonn +  $\Delta$  and the corresponding experimental values are given in the first three rows. The last four rows split the complete  $\Delta$  effect up into  $2N$  dispersion  $\Delta E_2$ , Fujita-Miyazawa type  $3N$  force effect  $\Delta E_3^{\text{FM}}$ , higher order  $3N$  force effect  $\Delta E_3^{\text{h.o.}}$ , and  $4N$  force effect  $\Delta E_4$  for  ${}^4\text{He}$ . All results are given in MeV.

the  $\sigma$ -meson exchange in  $v_{\Delta\Delta}$  that is not really constrained by elastic  $2N$  data; it could get constrained by the data in pionic channels coupling to  $2N$  channels above the inelastic threshold. The  $\sigma$ -meson exchange strength of the CD Bonn +  $\Delta$  potential was chosen to yield more binding in the  $3N$  system, and therefore its contribution to the binding energy of  ${}^4\text{He}$  is quite sizable as well. An alternative realistic coupled-channel potential with a weaker  $\sigma$ -meson in  $v_{\Delta\Delta}$  was developed in Ref. [24]. In the Appendix we show the differences relative to CD Bonn +  $\Delta$  and the corresponding predictions for  $3N$  and  $4N$  binding energies. (4) Finally, in contrast to the complete  $3N$  force contribution  $\Delta E_3^{\text{FM}} + \Delta E_3^{\text{h.o.}} = 3.55$  MeV, the contribution arising from the effective  $4N$  force  $\Delta E_4 = 0.17$  MeV is indeed rather small.

#### 4. Four-nucleon scattering

The  $n$ - ${}^3\text{H}$  and  $p$ - ${}^3\text{He}$  scattering is dominated by the total isospin  $\mathcal{T} = 1$  states while deuteron-deuteron ( $d$ - $d$ ) scattering by the  $\mathcal{T} = 0$  states; the  $n$ - ${}^3\text{He}$  and  $p$ - ${}^3\text{H}$  reactions involve both  $\mathcal{T} = 0$  and  $\mathcal{T} = 1$  states and are coupled to  $d$ - $d$  in  $\mathcal{T} = 0$ . All those reactions below three-body breakup threshold were calculated in Refs. [1,2,3]. Here we study the  $\Delta$ -isobar effect on the low-energy  $4N$  scattering observables.

In Fig. 7 we study the energy dependence of the total  $n$ - ${}^3\text{H}$  cross section. The  $\Delta$ -isobar excitation increases the  $3N$  binding energy and through scaling improves the description of the data around threshold. However, there is quite a significant non-beneficial  $\Delta$  effect in the region of the resonance which is strongly driven by  $n$ - ${}^3\text{H}$  relative  $P$  waves. In Table 2 we split this effect into  $2N$  dispersion,  $3N$  and  $4N$  force contributions, the last of which we find to be negligible. Furthermore, we split the total  $n$ - ${}^3\text{H}$  cross section  $\sigma_t$  into the  $S$ - and  $P$ -wave contributions  $\sigma_t^S$  and  $\sigma_t^P$ . As can be seen in Table 2, the  $\Delta$  effects on the  ${}^3\text{H}$  binding energy  $\epsilon_t$  and the  $S$ -wave cross section are correlated by scaling in the same way as it has been observed in Ref. [1], i.e.,  $\sigma_t^S$  decreases when  $\epsilon_t$  increases. In contrast, there is no

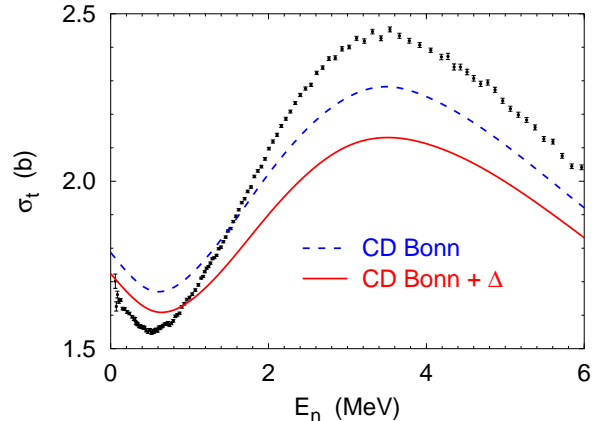


Fig. 7. Total cross section for  $n$ - ${}^3\text{H}$  scattering as function of neutron lab energy calculated with the CD Bonn (dashed curve) and CD Bonn +  $\Delta$  (solid curve) potentials. Experimental data are from Ref. [25].

	$\epsilon_t$	$\sigma_t^S$	$\sigma_t^P$	$\sigma_t$	$A_y^{\text{max}}$
CD Bonn	8.00	0.975	1.308	2.283	0.364
CD Bonn + $\Delta$	8.28	0.958	1.172	2.130	0.345
exp	8.48			2.450	
$2N$ dispersion	-0.51	0.036	-0.075	-0.039	-0.055
$3N$ force (FM)	0.50	-0.035	-0.058	-0.094	0.022
$3N$ force (h.o.)	0.29	-0.017	-0.004	-0.021	0.014
$4N$ force	< 0.001	< 0.001	< 0.001	< 0.001	< 0.001

Table 2

Separate  $\Delta$ -isobar effects on the observables of  $n$ - ${}^3\text{H}$  scattering at 3.5 MeV neutron lab energy.

such a correlation in  $P$  waves where both  $2N$  dispersion and effective  $3N$  force decrease the cross section while having opposite effects on  $\epsilon_t$ . This is different from  $3N$  scattering where the  $\Delta$  effect becomes visible, scaling aside, only at rather high energy, beyond 50 MeV in the center of mass (c.m.) system. At lower energies the individual  $\Delta$  contributions are not negligible, but very often cancel each other to a large extent. Much smaller effect on  $\sigma_t$  in the resonance region is observed in Refs. [14,15] where Urbana IX  $3N$  force is added to AV18.

In Fig. 8 we study the observables of  $p$ - ${}^3\text{He}$  scattering at 5.54 MeV proton lab energy. This reaction is related to  $n$ - ${}^3\text{H}$  by charge symmetry that is broken only by the Coulomb interaction and hadronic charge dependence. The charge-symmetric  $\Delta$  effect is therefore very similar in both reactions. It reduces the  $p$ - ${}^3\text{He}$  differential cross section at forward and backward angles increasing the discrepancy with data. It is small and non-beneficial for the proton analyzing power  $A_y$ , while the  $p$ - ${}^3\text{He}$  spin correlation coefficients remain described quite satisfactorily. Similar effects have also been observed in Ref. [17] using the Urbana IX  $3N$  force [10]. In the last column of Table 2 we split the  $\Delta$  effect into  $2N$ ,  $3N$  and  $4N$  contributions for the maximum values of  $A_y$  in  $n$ - ${}^3\text{H}$  scattering which is closely related to  $p$ - ${}^3\text{He}$   $A_y$ . The effects of the  $2N$  dispersion and effective  $3N$  force are quite sizable, about -15% and 10%, respectively, but par-

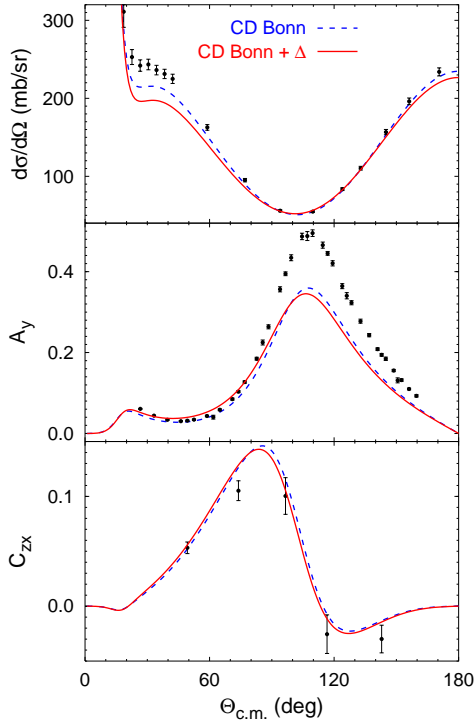


Fig. 8. Differential cross section, proton analyzing power  $A_y$  and  $p$ - ${}^3\text{He}$  spin correlation coefficient  $C_{zx}$  of  $p$ - ${}^3\text{He}$  scattering at 5.54 MeV proton lab energy as functions of c.m. scattering angle. Curves as in Fig. 7. The data are from Ref. [27] for the differential cross section and from Ref. [28] for the spin observables.

tially cancel each other. A similar canceling was observed in the  $3N$   $A_y$  [26] though there the  $3N$  force effect was larger than the  $2N$  dispersion, in contrast to the  $4N$  system.

The elastic differential cross section in the coupled  $p$ - ${}^3\text{H}$  and  $n$ - ${}^3\text{He}$  reactions correlates to some extent with that of  $p$ - ${}^3\text{He}$  and  $n$ - ${}^3\text{H}$  scattering and is similarly reduced by the  $\Delta$  excitation at forward and backward angles. In contrast, the effect is much weaker for the  $p + {}^3\text{H} \rightarrow n + {}^3\text{He}$  transfer cross section as shown in Fig. 9. The  $\Delta$  effect on  $A_y$  in this reaction is consistent with the findings of Ref. [3] where increasing the  $3N$  binding energy moves the predictions away from the data. The  $\Delta$  effect is tiny for the elastic  $d$ - $d$  cross section as shown in Fig. 10, but is visible for the deuteron tensor analyzing powers which, however, are very small.

As we found in Ref. [3] the observables of the two charge-symmetric transfer reactions  $d + d \rightarrow p + {}^3\text{H}$  and  $d + d \rightarrow n + {}^3\text{He}$  correlate to some extent with the  $3N$  binding energy and with the deuteron  $D$ -state probability. That former correlation is reflected in Fig. 11 where the inclusion of the  $\Delta$ -isobar excitation brings the theoretical predictions closer to the data for the differential cross section, but has a smaller effect on the analyzing powers.

## 5. Conclusions

The technical apparatus, developed in Refs. [1,2,3] for the solution of the  $4N$  bound state and scattering equa-

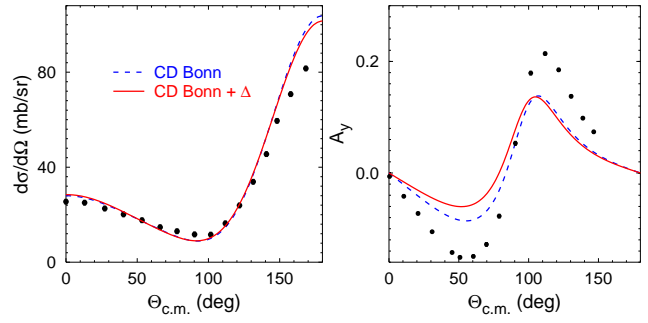


Fig. 9. Differential cross section and proton analyzing power of the  $p + {}^3\text{H} \rightarrow n + {}^3\text{He}$  reaction at 6 MeV proton lab energy. Curves as in Fig. 7. The cross section data are from Ref. [29].  $A_y$  data are from Ref. [30].

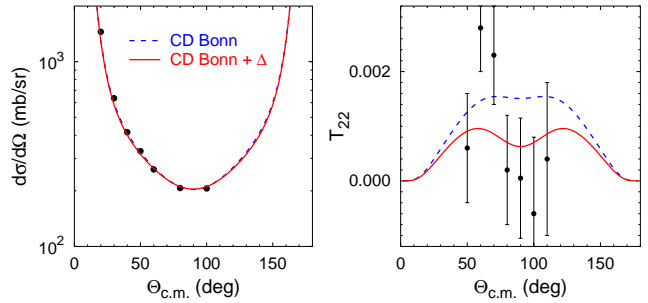


Fig. 10. Differential cross section and deuteron tensor analyzing power  $T_{22}$  of the elastic  $d$ - $d$  scattering at 3 MeV deuteron lab energy. Curves as in Fig. 7. The cross section data are from Ref. [31] and  $T_{22}$  data are from Ref. [32].

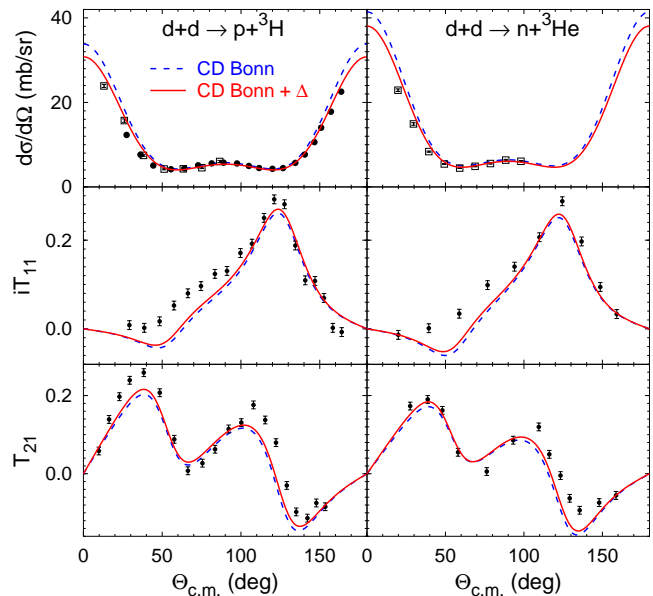


Fig. 11. Differential cross section and deuteron analyzing powers of the  $d + d \rightarrow p + {}^3\text{H}$  and  $d + d \rightarrow n + {}^3\text{He}$  reactions at 3 MeV deuteron lab energy. Curves as in Fig. 7. The cross section data are from Refs. [33] (squares) and [34] (circles). Analyzing power data are from Ref. [34] for  $d + d \rightarrow p + {}^3\text{H}$  and from Ref. [35] for  $d + d \rightarrow n + {}^3\text{He}$ .

tions, is employed and extended. The extension covers the use of a realistic coupled-channel potential allowing for the excitation of a single nucleon to a  $\Delta$  isobar. The  $\Delta$  isobar mediates effective  $2N$ ,  $3N$  and  $4N$  forces, consistent with each other. A procedure for isolating the  $\Delta$ -isobar effects of  $2N$ ,  $3N$  and  $4N$  nature on observables is given and used to study different dynamic mechanisms.

*Technically*, this paper demonstrates that  $4N$  calculations with realistic  $2N$ ,  $3N$  and  $4N$  forces are feasible. The Coulomb repulsion between protons is included. Fully converged results for the  $4N$  binding energy and for the  $4N$  scattering observables below three-body breakup threshold are obtained.

*Physicwise*, this paper shows for the first time that, within the present model space,  $4N$  force effect on nuclear observables is much smaller than the  $3N$  force effect. That fact is shown in the framework of  $\Delta$ -mediated effective many-body forces for the  $4N$  bound state and low-energy scattering observables, and is a very valuable confirmation of the traditional belief in a hierarchic order for the importance of many-nucleon forces. However, the inclusion of the  $\Delta$  isobar is unable to resolve the long-standing discrepancies with the experimental data, neither for the  $n$ - $^3\text{H}$  total cross section in the resonance region nor for  $A_y$  in  $p$ - $^3\text{He}$  scattering. Nevertheless, in addition to possible differences resulting from model dependence, some differences between the work of Lazauskas & Carbonell [14], the Pisa group [16,17] and the present calculations need to be sorted out in the near future. While our findings seem to coincide with those of the Pisa group for  $p$ - $^3\text{He}$  vis-a-vis the effect of the  $3N$  force, the calculations by Lazauskas & Carbonell indicate that the Urbana IX  $3N$  force, when added to AV18  $2N$  force, bears almost no effect on the total cross section  $\sigma_t$  in the  $n$ - $^3\text{H}$  resonance region. Given that  $n$ - $^3\text{H}$  and  $p$ - $^3\text{He}$  only differ by the Coulomb interaction and small charge dependent terms in the  $2N$  force, one does not expect such a different behavior between  $n$ - $^3\text{H}$  and  $p$ - $^3\text{He}$  when  $3N$  forces are added.

*Dynamically*, our calculations are based on the two-baryon coupled-channel potential CD Bonn +  $\Delta$  [13], which fits the deuteron properties and  $2N$  elastic scattering data as well as the best  $2N$  potentials [4,5,6,7]. As standard in the description of nuclear structure and scattering, the  $\Delta$  isobar is assumed to be a stable particle of fixed mass without subthreshold corrections arising from the  $\Delta$ -generated  $P_{33}$   $\pi N$  resonance. This assumption is a crude and in principle unnecessary simplification of the  $\Delta$  isobar's dynamic structure, not allowing a direct application of the coupled-channel potential to pionic reactions. This fact is the reason why the  $\Delta N$  and especially the  $\Delta\Delta$  parts of the two-baryon potential in its present form are not sufficiently constrained by the  $2N$  data; their full determination requires the data of  $\pi NN$  dynamics. We recall that all nuclear potentials are indeterminate to some extent, e.g.,  $2N$  potentials with respect to their short-range behavior and their amount of nonlocality. However we are especially concerned about the indeterminacy of the  $\Delta\Delta$

part of the employed two-baryon coupled-channel potential, since it is responsible for the higher-order  $3N$  force and for the  $4N$  force, the focus of this paper. Fortunately, that dynamic indeterminacy does not change our physics conclusion in any form: Exploiting that model dependence of the potential by using, besides CD Bonn +  $\Delta$ , also its alternative CD Bonn +  $\Delta'$  described in the Appendix, the  $4N$  force effect on binding energy remains much smaller than the  $3N$  force effect and for the scattering observables it is completely negligible. Finally, completing the list of all possible shortcomings of the employed two-baryon coupled-channel potential, the  $2N$  potential in the presence of a  $\Delta$  isobar, encountered in the Hamiltonian underlying our calculations, is constrained only by the data of  $\pi NN$  dynamics; however, different choices for that part of the potential appear inconsequential for all studied observables according to our findings in the  $3N$  system.

*In a longer range vision*, the extension of the Hamiltonian of this paper to cover also pionic reactions is quite possible, pushing the descriptions of  $3N$  and  $4N$  scattering to intermediate energies and thereby decreasing the model dependence inherent in the chosen force model with  $\Delta$ -isobar excitation. Furthermore, we hope for a consistent derivation and tuning of purely nucleonic  $2N$ ,  $3N$  and  $4N$  forces in the framework of chiral EFT; their subsequent application to the  $4N$  observables, studied in this paper, would be a challenging enterprise and a wonderful alternative to our present work.

We thank R. Lazauskas and M. Viviani for the discussion of  $3N$  force effects. A.D. is supported by the Fundação para a Ciência e a Tecnologia (FCT) grant SFRH/BPD/34628/2007 and A.C.F. in part by the FCT grant POCTI/ISFL/2/275.

## Appendix A. Alternative two-baryon coupled-channel potential CD Bonn + $\Delta'$

This paper works predominantly with the two-baryon coupled-channel potential CD Bonn +  $\Delta$ , derived in Ref. [13]. Its particular feature is a strong  $\sigma$ -meson coupling  $g_{\sigma NN}g_{\sigma\Delta\Delta}/4\pi = 8.7$  for the direct  $v_{\Delta\Delta}$  component in  $N\Delta$  states  $^5SDG_2$  coupled to the nucleonic partial wave  $^1D_2$ . That coupling is undetermined within sizable limits; it was chosen to obtain more binding in the  $3N$  bound state, nevertheless allowing for the optimal fit of  $\chi^2/\text{datum} = 1.02$  to the elastic  $2N$  scattering data. This appendix presents selected results for an alternative coupled-channel potential CD Bonn +  $\Delta'$  [24] with weaker  $g_{\sigma NN}g_{\sigma\Delta\Delta}/4\pi = 5.0$  that, after refitting the parameters of the two  $\sigma$  mesons in the nucleonic part  $v_{NN}$  of the potential, still allows for an optimal description of  $2N$  data with  $\chi^2/\text{datum} = 1.02$ . For completeness in Table A.1 we give the changed  $\sigma$ -meson parameters of the CD Bonn +  $\Delta'$  potential in the  $^1D_2$  partial wave; other parameters have the same values as for CD Bonn +  $\Delta$  and are given in Ref. [13].

Table A.2 shows the changes in the binding energy of

	$m_{\sigma_i}$	$g_{\sigma_i}^2/4\pi (pp)$	$g_{\sigma_i}^2/4\pi (np)$	$g_{\sigma_i}^2/4\pi (nn)$
$\sigma_1$	350	0.50683	0.51269	0.51424
$\sigma_2$	1225	148.10	148.42	149.28

Table A.1

$\sigma$ -meson parameters for the potential CD Bonn +  $\Delta'$  in the nucleonic partial wave  $^1D_2$ . The masses  $m_{\sigma_i}$  are in MeV.

$^3\text{H}$ ,  $^3\text{He}$  and  $^4\text{He}$  arising for CD Bonn +  $\Delta'$ . The  $\Delta$ -isobar effect is weaker than for CD Bonn +  $\Delta$ , turning even non-beneficial for  $^4\text{He}$ . Whereas the  $2N$  dispersive and  $3N$  Fujita-Miyazawa effects, i.e.,  $\Delta E_2$  and  $\Delta E_3^{\text{FM}}$ , remain practically unchanged, the higher order  $3N$  and  $4N$  force contributions, i.e.,  $\Delta E_3^{\text{h.o.}}$  and  $\Delta E_4$ , being much more sensitive to the  $v_{\Delta\Delta}$  component, get strongly reduced, thereby changing the complete  $\Delta$ -isobar effect considerably. This is a measure of our model dependence for  $0.17 > \Delta E_4 > 0.03$ .

	$^3\text{H}$	$^3\text{He}$	$^4\text{He}$
CD Bonn	8.00	7.26	26.18
CD Bonn + $\Delta'$	8.05	7.31	25.89
exp	8.48	7.72	28.30
$\Delta E_2$	-0.51	-0.48	-2.78
$\Delta E_3^{\text{FM}}$	0.50	0.48	2.20
$\Delta E_3^{\text{h.o.}}$	0.06	0.05	0.26
$\Delta E_4$			0.03

Table A.2

Same as Table 1, but with CD Bonn +  $\Delta'$ .

- [18] A. Deltuva, A. C. Fonseca, P. U. Sauer, Phys. Rev. C 71 (2005) 054005.
- [19] A. Deltuva, A. C. Fonseca, P. U. Sauer, Phys. Rev. C 72 (2005) 054004.
- [20] J. Fujita, H. Miyazawa, Prog. Theor. Phys. 17 (1957) 360.
- [21] H. Kamada, W. Glöckle, Nucl. Phys. A548 (1992) 205.
- [22] P. Grassberger, W. Sandhas, Nucl. Phys. B2 (1967) 181, ; E. O. Alt, P. Grassberger, and W. Sandhas, JINR report No. E4-6688 (1972).
- [23] A. Deltuva, K. Chmielewski, P. U. Sauer, Phys. Rev. C 67 (2003) 054004.
- [24] A. Deltuva, L. P. Yuan, J. Adam Jr., P. U. Sauer, Phys. Rev. C 70 (2004) 034004.
- [25] T. W. Phillips, B. L. Berman, J. D. Seagrave, Phys. Rev. C 22 (1980) 384.
- [26] A. Deltuva, K. Chmielewski, P. U. Sauer, Phys. Rev. C 67 (2003) 034001.
- [27] D. G. McDonald, W. Haeberli, L. W. Morrow, Phys. Rev. 133 (1964) B1178.
- [28] M. T. Alley, L. D. Knutson, Phys. Rev. C 48 (1993) 1890.
- [29] W. E. Wilson, R. L. Walter, D. B. Fossan, Nucl. Phys. 27 (1961) 421.
- [30] J. J. Jarmer, R. C. Haight, J. E. Simmons, J. C. Martin, T. R. Donoghue, Phys. Rev. C 9 (1974) 1292.
- [31] J. M. Blair, G. Freier, E. Lampi, W. Sleator, J. H. Williams, Phys. Rev. 74 (1948) 1594.
- [32] B. J. Crowe, C. R. Brune, W. H. Geist, H. J. Karwowski, E. J. Ludwig, K. D. Veal, A. C. Fonseca, G. M. Hale, K. A. Fletcher, Phys. Rev. C 61 (2000) 034006.
- [33] J. M. Blair, G. Freier, E. Lampi, W. Sleator, J. H. Williams, Phys. Rev. 74 (1948) 1599.
- [34] W. Gruebler, V. König, P. A. Schmelzbach, R. Risler, R. E. White, P. Marmier, Nucl. Phys. A193 (1972) 129.
- [35] L. J. Dries, H. W. Clark, R. Detomo, T. R. Donoghue, Phys. Lett. 80B (1979) 176.

## References

- [1] A. Deltuva, A. C. Fonseca, Phys. Rev. C 75 (2007) 014005.
- [2] A. Deltuva, A. C. Fonseca, Phys. Rev. Lett. 98 (2007) 162502.
- [3] A. Deltuva, A. C. Fonseca, Phys. Rev. C 76 (2007) 021001(R).
- [4] R. B. Wiringa, V. G. J. Stoks, R. Schiavilla, Phys. Rev. C 51 (1995) 38.
- [5] R. Machleidt, Phys. Rev. C 63 (2001) 024001.
- [6] P. Doleschall, Phys. Rev. C 69 (2004) 054001.
- [7] D. R. Entem, R. Machleidt, Phys. Rev. C 68 (2003) 041001(R).
- [8] H. T. Coelho, T. K. Das, M. R. Robilotta, Phys. Rev. C 28 (1983) 1812.
- [9] S. A. Coon, M. D. Scadron, P. C. McNamee, B. R. Barrett, D. W. E. Blatt, B. H. J. McKellar, Nucl. Phys. A317 (1979) 242.
- [10] B. S. Pudliner, V. R. Pandharipande, J. Carlson, S. C. Pieper, R. B. Wiringa, Phys. Rev. C 56 (1997) 1720.
- [11] U. van Kolck, Prog. Part. Nucl. Phys 43 (1999) 337.
- [12] E. Epelbaum, W. Glöckle, U.-G. Meissner, Nucl. Phys. A671 (2000) 295.
- [13] A. Deltuva, R. Machleidt, P. U. Sauer, Phys. Rev. C 68 (2003) 024005.
- [14] R. Lazauskas, J. Carbonell, Phys. Rev. C 70 (2004) 044002.
- [15] R. Lazauskas, J. Carbonell, A. C. Fonseca, M. Viviani, A. Kievsky, S. Rosati, Phys. Rev. C 71 (2005) 034004.
- [16] M. Viviani, A. Kievsky, S. Rosati, E. A. George, L. D. Knutson, Phys. Rev. Lett. 86 (2001) 3739.
- [17] B. M. Fisher, C. R. Brune, H. J. Karwowski, D. S. Leonard, E. J. Ludwig, T. C. Black, M. Viviani, A. Kievsky, S. Rosati, Phys. Rev. C 74 (2006) 034001.